# Multi-angle Imaging SpectroRadiometer (MISR) Aerosol Optical Depth over Land (F12_0022) Technical Document

## 1. Intent of This Document

This document is intended for users who wish to compare satellite-derived observations with climate model output in the context of the CMIP5/IPCC experiments. It summarizes essential information needed for comparing this dataset to climate model output. References and useful links are provided.

This dataset is provided as part of an effort to increase the usability of NASA satellite observational data for the modeling and model analysis communities. This is not a standard NASA satellite instrument product, but does represent an effort on behalf of data experts to identify a product that is appropriate for routine model evaluation. These data have been reprocessed, reformatted, and created solely for comparisons with climate model output. Community feedback to improve and validate the dataset for modeling usage is appreciated. Email comments to HQ-CLIMATE-OBS@mail.nasa.gov.

*Dataset Filename*:

od550aer_MISR_L3_F12_0022_200003-201211.nc

*Ancillary Filenames:*

od550aerNobs_MISR_L3_F12_0022_200003-201211.nc,
od550aerStddev_MISR_L3_F12_0022_200003-201211.nc

*Technical Point of Contact:*

Arlindo da Silva, NASA Goddard Space Flight Center, arlindo.dasilva@nasa.gov
Ralph Kahn, NASA Goddard Space Flight Center, ralph.a.kahn@nasa.gov

## 2. Data Origin and Field Description

MISR (Multi-angle Imaging SpectroRadiometer) is a key instrument aboard the Terra satellite (launched in December 1999) in a sun-synchronous orbit. MISR provides new types of information for scientists studying Earth's climate, such as the partitioning of energy and carbon between the land surface and the atmosphere, and the regional and global impacts of different types of atmospheric particles and clouds on climate. The change in reflection at different view angles affords the means to distinguish different types of atmospheric particles (aerosols), cloud forms, and land surface covers. Combined with stereoscopic techniques, this enables construction of 3-D models and estimation of the total amount of sunlight reflected by Earth's diverse environments. MISR acquires systematic multi-angle imagery for global monitoring of top-of-atmosphere and surface albedos and to measure the shortwave radiative properties of aerosols, clouds, and surface scenes in order to characterize their impact on the Earth's climate.

The Terra satellite orbit is timed so that daytime descending passes (from north to south) cross the equator in the morning (10:30 LT). This orbit, with a 16-day repeat cycle on the World Reference System (WRS-2) grid, is precisely controlled and has remained extremely stable in both space and time over the mission to date. With a ~400 km swath, the MISR instrument views the entire Earth's surface every 9 days, with repeat coverage between 2 and 9 days depending on latitude. MISR acquires data in 4 spectral channels (blue, green, red, and near-infrared) with 9 push-broom cameras providing 5 viewing angles (0, 26.1, 45.6, 60.0, and 70.5 degrees.) See Section 6 for an overview of the MISR instrument.

The pixel-level (Level-2) MISR aerosol product (archived product file name prefix *MISR_AM1_AS_AEROSOL*) is at a nominal native spatial resolution of 17.6 km. For CMIP5, monthly aerosol optical depth retrievals at 550 nm (averaged from daytime orbits) are provided over land and cover the time period from March 2000 through a recently available processed month (November 2012 at the time of this writing). In producing these monthly means, we filtered out retrievals over water and permanent ice according to surface characterization from the IGBP (International Geosphere-Biosphere Program) dataset. The product contains temporal and geometric coordinate variables (time, latitude, and longitude) along with the mean aerosol optical depth. The time corresponds to the 16th day of the month and is given as the number of days since March 1, 2000. The latitude and longitude grid is equal-angle at 1° resolution. The longitude grid center range is from 0.5 to 359.5 degrees while the latitude extends from -89.5 to +89.5 degrees (south to north). The value of aerosol optical depth is positive and non-dimensional and is equivalent to values provided at 558 nm (MISR green band) by the Science Data Set named *RegBestEstimateSpectralOptDepth* in the archived *MISR_AM1_AS_AEROSOL* Hierarchical Data Format (HDF) file available through the Atmospheric Sciences Data Center at NASA's Langley Research Center.

| | |
|---|---|
| CF variable name, units | **Long_Name:** Ambient Aerosol Optical Thickness at 550 nm<br>**Standard Name:** atmosphere_optical_thickness_due_to_ambient_aerosol<br>**Units:** dimensionless |
| Spatial resolution | 1° equal angle |
| Temporal resolution | Monthly average, from March 2000–December 2012 |
| Coverage | Global |

The dataset includes two ancillary files. File named *od550aerStdv_MISR_L3_F12_0022_200003-201212.nc* provides the standard deviation of the individual observations used to compute the monthly average, for each equal-angle 1° grid-box. File named *od550Nobs_MISR_L3_F12_0022_200003-201212.nc* gives the total monthly counts for all pixels included in each 1° grid-box.

## 3. Data Product Algorithm Overview

The MISR Standard Aerosol Retrieval Algorithm reports aerosol optical depth (AOD) and aerosol type derived over 17.6 km x17.6 km retrieval regions, derived from MISR top-of-atmosphere (TOA) radiances measured in 1.1 km sub-regions within each region (Martonchik *et al.* 1998, 2002, 2009). Separate algorithms are used over dark water and heterogeneous land, in a 3-stage process (Diner *et al.* 2006; Kahn et al., 2009b). Stage 1 involves the processing of radiometrically and geometrically calibrated radiances, performing ozone and water vapor corrections. Screening is also performed in Stage 1 for cloudy and missing radiance data, complex terrain over land, low solar zenith angle and sun glint contaminated pixels over water. The last step in Stage 1 converts the remaining radiance data to equivalent reflectances. In Stage 2 a determination is made about the appropriate algorithm to be use (land or water), and the data are processed accordingly. In Stage 3, acceptance criteria are utilized to match simulated top-of-atmosphere equivalent reflectances from look-up tables with those reflectances observed by the instrument.

The over-land algorithm is a two-step process that takes full advantage of the multi-angle characteristics of the MISR instrument (Martonchik *et al.* 2009). As part of Step 1, under the assumption that the angular signature of surface reflectance is spectrally invariant, aerosol models are selected from a pre-determined collection, eliminating those aerosol mixtures that grossly disagree with the observed radiances (Diner *et al.* 2005). Subsequently, an empirical orthogonal function analysis is performed on the remaining pixels to separate the surface and atmosphere contributions to the TOA reflectances. The aerosol optical depth is determined so as to minimize the difference between the observed and reconstructed atmospheric reflectances. Details of the algorithm can be found in Martonchik *et al.* (2009).

Critical to the success of the procedure outlined above is providing the algorithm with realistic aerosol optical model models and mixture options at a level of detail consistent with the sensitivity of the measurements. A combination of theoretical sensitivity studies, field campaign results, and statistical comparisons with surface in-situ measurements has been used to develop the aerosol optical models used by the standard MISR algorithm (Kahn *et al.* 2001, 2005, 2009b; Chen *et al.* 2008; Kalashkova and Kahn 2006).

## 4. Validation and Uncertainty Estimates

The Level 2 MISR aerosol optical depth parameter (*RegBestEstimateSpectralOptDepth)* used for constructing the monthly mean files is considered *Stage 3 Validated* maturity level for Version 22. This applies to aerosol optical depth over both water and land, which are produced using different retrieval approaches (Martonchik *et al*. 2009, and references therein.)

A global comparison of retrieved aerosol optical depths for coincident MISR and AERONET data was performed for the time period December 2000 through November 2002 for the early post-launch version of the MISR aerosol product (Kahn *et al*. 2005a). The comparison shows that overall, about two-thirds of the MISR-retrieved aerosol optical depth (AOD) values in the green band fall within 0.05 or 20% × AOD measured by AERONET, and about 40% are within 0.03 or 10% × AOD. As expected, correlation coefficients are highest for maritime cases (~0.9), and lowest for bright desert sites (still greater than ~0.7). Additional MISR optical depth validation, yielding similar results, has been performed over bright deserts (Martonchik *et al.* 2004, Christopher and Wang 2004; Kalashnikova and Kahn, 2006), over the continental United States (Liu *et al.* 2004, 2007), over coastal water (Redemann *et al*. 2005, Schmid *et al*, 2003, Reidmiller *et al*. 2006), over biomass burning sites (Chen *et al.* 2008), over north India aerosol pollution (DiGirolamo *et al*. 2004), and using sun photometer data to evaluate MISR and MODIS results over land and water (Abdou *et al*., 2005.) The impact on MISR and MODIS retrieved AOD and aerosol properties of algorithm surface boundary condition and particle property assumptions, calibration, sampling, and other factors over dark water is given in Kahn *et al.* (2007b)

A comprehensive statistical approach to assess the quality of MISR aerosol products Version 22 can be found in Kahn *et al.* (2010). Overall, about 70% to 75% of MISR AOD retrievals fall within 0.05 or 20% × AOD of the paired validation data from the Aerosol Robotic Network (AERONET), and about 50% to 55% are within 0.03 or 10% × AERONET AOD, except at sites where dust or mixed dust and smoke are commonly found.

## 5. Consideration for Model-Observation Comparisons

Satellite observations are the only means by which the global aerosol field can be systematically observed. Aerosol climatologies from current and heritage satellite data records differ in magnitude and monthly variability. These differences are due to a number of reasons: types of orbit, spatial resolution, diurnal sampling, spectral resolution and placement, satellite viewing geometry, cloud contamination, proper knowledge of surface characteristics, etc. In contrast to the spectrally-and/or spatially-challenged heritage data records, MISR contains 4 spectral bands with a nominal 275 m spatial resolution at nadir, 1.1 km for all off-nadir views, from 9 cameras viewing at nine different angles. This combination of spectral, viewing angles and spatial resolution allow for better detection of cloud and surface characteristics with fewer algorithmic assumptions.

The monthly dataset described in this Technical Note set is derived from Version F12_0022 MISR Level-2 files, monthly averaged to a 1 degree grid, eliminating data over water and permanent ice; no other processing has been applied to the data. The MISR aerosol optical depth product over land tends to be the highest quality such data set currently available (Kinne, 2008). Although MISR aerosol optical depth retrievals are also available over ocean, the more frequent coverage provided by the MODIS-derived aerosol optical depth over ocean (obs4MIPS dataset *od550aer_MODIS_L3_C5*) is likely to produce a more statistically robust monthly sample.

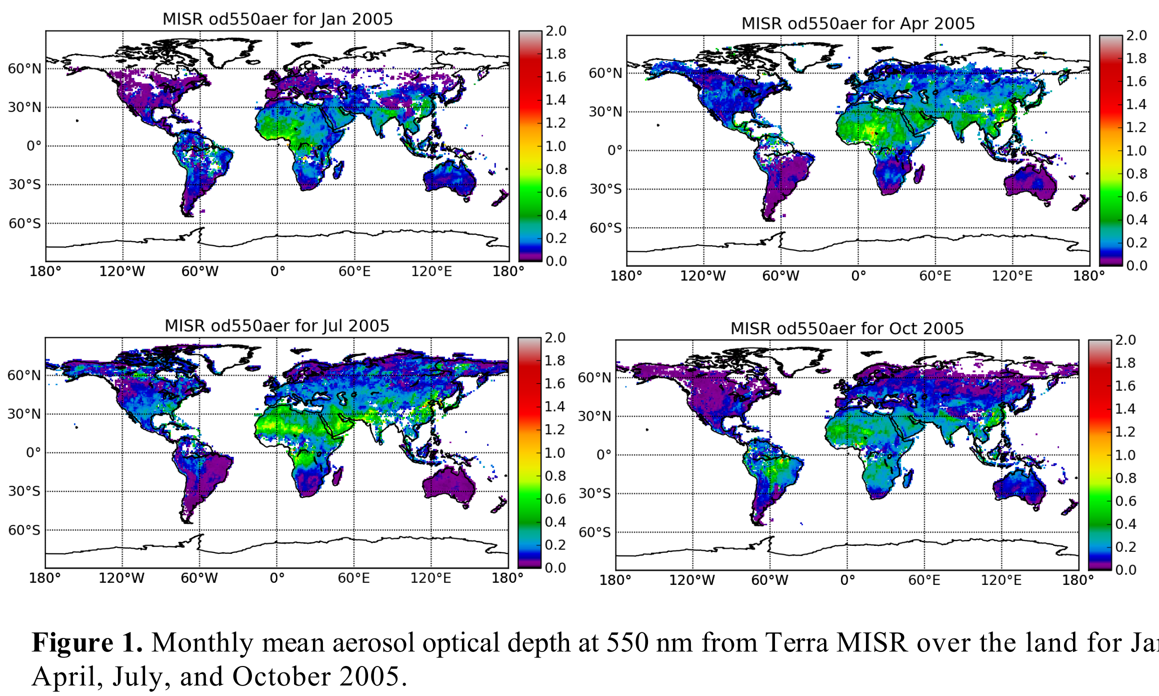


**Figure 1.** Monthly mean aerosol optical depth at 550 nm from Terra MISR over the land for January, April, July, and October 2005.

### 5.1 Monthly AOD Distribution Example

Sample monthly mean aerosol optical depth at 550 nm from MISR is shown in Fig. 1 for four months in 2005. The aerosol seasonal cycle is apparent, with Saharan dust peaking in the spring and summer months, biomass burning being stronger in South America in October and predominant in equatorial Africa in July. Anthropogenic aerosols in the Northern hemisphere reach a peak in the summer months associated with high temperature, pressure, and humidity values and increased particle hygroscopic growth. Notice that increased aerosol optical depth in Siberia, Alaska, and Canada induced by seasonal boreal fires. Movies with the monthly mean, standard deviation and number observations for each month in this dataset is available on-line at

ftp://gmaoftp.gsfc.nasa.gov/pub/data/dasilva/obs4MIPS/od550aer_MISR_L3_F12_0022/

### 5.2 Asynoptic Time Sampling

Because Terra satellite operates in a sun-synchronous polar orbit, it samples in the visible at relatively constant local solar time at each location (i.e., ~10:30 local at the equator) so it cannot resolve the diurnal cycle. In contrast, typical model monthly averaged outputs contain the averaged values over a time series of data within a fixed time interval (e.g., every 6 hours). For many constituents in the upper atmosphere, this difference is not likely a problem, although for regions influenced by deep convection and its modulation of the diurnal cycle (e.g., tropical land masses), wildfire activity that tends to peak in the mid-afternoon, photochemical smog that can have one or two diurnal peaks, and other diurnal variability in natural and anthropogenic emissions, the potential impact of time sampling bias should be considered.

### 5.3 Inhomogeneous Sampling

Because the monthly averaged value in this MISR data product is an average over observational data available in a given grid cell, the number of samples used for averaging varies with the geo-location of the cell. Because of the convergence of longitude lines near the poles, the frequency, as well as the range of times-of-day when data are collected broadens as one moves from the equator toward either pole, with sampling at a given location as often as once every two days. Because the increased number of overpasses near the poles occurs over a broader portion of the diurnal cycle, this can affect the amplitude of the observed diurnal cycle in high-latitudes relative to the mid-latitudes and tropics. However, persistent cloudiness, a smaller-amplitude diurnal cycle in general, low sun-zenith angle, and polar night also affect high-latitude sampling. Therefore, the entire MISR data set cannot be treated as uniformly sampled at 10:30 local time. The ancillary files with the observation count and standard deviations for each grid can be useful to quantify the inhomogeneous sampling of the dataset.

### 5.4 Clear-sky Sampling

Because MISR (and all other total-column remote sensing) aerosol optical depth retrievals are only possible under clear sky conditions, there is a *Fair Weather Bias*. For hygroscopic aerosols, clear sky conditions are often associated with subsidence and lower values of relative humidity leading to smaller values of aerosol optical depth. Furthermore, clear-sky conditions following a rainstorm will be associated with reduced aerosol optical depth values due the wash out process induced by precipitation. Whenever possible, model aerosol optical estimates should take into consideration cloud fraction and humidity conditions within the clear portions of the grid-box.

## 6. Instrument Overview

MISR, the Multi-angle Imaging SpectroRadiometer instrument, was successfully launched into sun-synchronous polar orbit aboard Terra, NASA's first Earth Observing System (EOS) spacecraft, on December 18, 1999. First light for the MISR instrument occurred on February 24, 2000. MISR measurements are designed to improve our understanding of the Earth's environment and climate. Viewing the sunlit Earth simultaneously at nine widely spaced angles in each of four spectral bands, MISR provides radiometrically and geometrically calibrated quantitative image data. A summary of the MISR instrument characteristics is given in the table below.

**MISR Instrument Description**

| Parameter | Value | Characteristics |
|---|---|---|
| Camera View Zenith Angles at Earth's Surface | 0.0 ° (nadir), 26.1, 45.6, 60.0 and 70.5 ° (both fore and aft of nadir) | 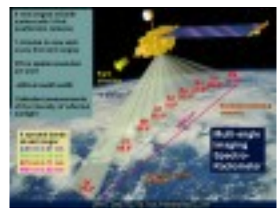<br>*Global Mode:*<br>- 275m sampling in all nadir bands<br>- 275m sampling in red band of off-nadir cameras<br>- 1.1km for other channels<br>*Local Mode (targeted):*<br>- 275m all channels all cameras |
| Swath Width | Approximately 400 kilometers (249 miles) (9-day global coverage; 2 days near the poles) | |
| Cross-Track x Along-Track Pixel Sampling | 275 x 275 meters (902 x 902 feet)<br>1.1 x 1.1 kilometers (0.68 x 0.68 mile) | |
| Spectral Bands (Solar Spectrum Weighted) | 446.4, 557.5, 671.7, 866.4 nanometers | |
| Spectral Bandwidths | 41.9, 28.6, 21.9, 39.7 nanometers | |

For more details on the MISR instrument and project, see the MISR web site, the MISR Project Guide, and the MISR Experiment Overview. For details on MISR results, see the MISR publications page. For additional information on the MISR instrument see Diner *et al*. (2002).

*Acknowledgements*. Special thanks to the MISR science and instrument teams.

## 7. References

Abdou, W.A., D.J. Diner, J.V. Martonchik, C.J. Bruegge, R.A. Kahn, B.J. Gaitley, K.A. Crean, L.A. Remer, and B. Holben, 2005, Comparison of coincident MISR and MODIS aerosol optical depths over land and ocean scenes containing AERONET sites, J. Gelphys. Res., doi:10.1029/2004JD004693.

Chen, W-T, R. Kahn, D. Nelson, K. Yau, and J. Seinfeld, 2008, Sensitivity of multi-angle imaging to optical and microphysical properties of biomass burning aerosols, J. Geophys. Res. 113, D10203, doi:10.1029/2007JD009414.

Christopher, S.. and J. Wang, 2004, Intercompason between multi-angle imaging spectroradiometer (MISR) and sunphotometer aerosol optical thickness in dust source regions of China, implications for satellite aerosol retrievals and radiative forcing calculations, Tellus 56B, 451-456.

Di Girolamo, L., and M.J. Wilson, 2003. A first look at band-differenced angular signatures for cloud detection from MISR. IEEE Trans. Geosci. Remote Sens. 41, 1730-1734.

DiGirolamo, L., T.C. Bond. D. Bramer. D.J. Diner, F. Fettinger, R.A. Kahn, J.V. Martonchik, M.V. Ramana, V. Ramanathan, and P.J. Rasch, 2004, Analysis of Multi-angle Imaging SpectroRadiometer (MISR) aerosol optical depths over greater India during winter 2001-2004, Geophys. Res. Let., 31, L23115, doi:10.1029/2004GL021273.

Diner, D. J. et al. "Performance of the MISR Instrument During Its First 20 Months in Earth Orbit", *IEEE. Trans. Geosci. Rem. Sens.* 40 (7), 1449-1466 (July 2002).

Diner, D.J., J.V. Martonchik, R.A. Kahn, B. Pinty, N. Gobron, D.L. Nelson, and B.N. Holben, 2005. Using angular and spectral shape similarity constraints to improve MISR aerosol and surface retrievals over land. Rem. Sens. Environ. 94, 155-171.

Diner, D.J., R.A. Kahn, C.J. Bruegge, J.V. Martonchik, W.A. Abdou, B.J. Gaitley, M.C. Helmlinger, O.V. Kalashnikova, and W-H. Li (2004). Refinements to MISR's radiometric calibration and implications for establishing a climate-quality aerosol observing system. Proc. SPIE 5652, 57-65.

Diner, D.J., W. Abdou, T. Ackerman, K. Crean, H. Gordon, R. Kahn, J. Martonchik, S. McMuldroch, S. Paradise, B. Pinty, M. Verstrete, M. Wang, and R. West, MISR Level 2 Aerosol Retrieval Algorithm Theoretical Basis, JPL- D11400, Rev. E, 2001.

Hu et al.,Performance of the MISR LAI and FPAR Algorithm: A Case Study in Africa. Remote Sens. Environ, Vol. 88, Issue 3, 15 December 2003, pp. 324-340 (PDF).

Kahn, R., W-H. Li, J. Martonchik, C. Bruegge, D. Diner, B. Gaitley, W.Abdou, O. Dubovik, B. Holben, S. Smirnov, Z. Jin, and D. Clark, 2005b. MISR low-light-level calibration, and implications for aerosol retrieval over dark water, J. Atmosph, Sci. 62, 1032-1062.

Kahn, R., B. Gaitley, J. Martonchik, D. Diner, K. Crean, and B. Holben, 2005a, MISR global aerosol optical depth validation based on two years of coincident AERONET observations, J. Geophys. Res., doi:10:1029/2004JD004706

Kahn, R., J. Anderson, T.L. Anderson, T. Bates, F. Brechtel, C.M. Carrico, A. Clarke, S.J. Doherty, E. Dutton, R. Flagan, R. Frouin, H. Fukushima, B. Holben, S. Howell, B. Huebert, A. Jefferson, H. Jonsson, O. Kalashnikova, J. Kim, S-W. Kim, P. Kus, W-H. Li, J.M. Livingston, C. McNaughton, J. Merrill, S. Mukai, T. Murayama, T. Nakajima, P. Quinn, J. Redemann, M. Rood, P. Russell, I. Sano, B. Schmid, J. Seinfeld, N. Sugimoto, J. Wang, E.J. Welton, J-G. Won, S-C. Yoon, 2004. Environmental Snapshots From ACE-Asia, J. Geophys. Res., doi:2003jd004339.

Kahn, R., P. Banerjee, and D. McDonald, 2001a. "The Sensitivity of Multiangle Imaging to Natural Mixtures of Aerosols Over Ocean", J. Geophys. Res.106, 18219-18238.

Kahn, R., P. Banerjee, D. McDonald, and J. Martonchik, "Aerosol Properties Derived from Aircraft Multi-angle Imaging Over Monterey Bay", J. Geophys. Res.106, 11977-11995, 2001b.

Kahn, R., P. Banerjee, D. McDonald, and D. Diner, 1998, "Sensitivity of Multiangle imaging to

Aerosol Optical Depth, and to Pure- Particle Size Distribution and Composition Over Ocean", J. Geophys. Res. 103, 32,195-32,213.

Kahn, R., Y. Chen, D.L. Nelson, F-Y. Leung, Q. Li, D.J. Diner, and J.A. Logan, 2008. Wildfire smoke injection heights - Two perspectives from space, Geophys. Res. Lett. 35, doi:10.1029/2007GL032165.

Kahn, R. A., M. J. Garay, D. L. Nelson, K. K. Yau, M. A. Bull, B. J. Gaitley, J. V. Martonchik, and R. C. Levy (2007b). Satellite-derived aerosol optical depth over dark water from MISR and MODIS: Comparisons with AERONET and implications for climatological studies. J. Geophys. Res., 112, D18205, doi:10.1029/2006JD008175.

Kahn, R., A. Petzold, M. Wendisch, E. Bierwirth, T. Dinter, M. Esselborn, M. Fiebig, B. Heese, P. Knippertz, D. Muller, A. Schladitz, and W. von Hoyningen-Huene, 2009. Desert Dust Aerosol Air Mass Mapping in the western Sahara, Using particle properties derived from space-based multi-angle imaging, *Tellus 61B*, 239-251, doi:10.1111/j.1600-0889.2008.00398.x..

Kahn, R.A., D.L. Nelson, M. Garay, R.C. Levy, M.A. Bull, D.J. Diner, J.V. Martonchik, S.R. Paradise, and E.G. Hansen, and L.A. Remer, 2009. MISR Aerosol product attributes, and statistical comparisons with MODIS. IEEE Trans. Geosci. Remt. Sens 47, 4095-4114.

Kahn, R., R. West, D. McDonald, B. Rheingans, and M.I. Mishchenko, 1997. Sensitivity of Multi-angle remote sensing observations to aerosol sphericity, J. Geophys. Res., 102, 16861-16870.

Kahn, R. A., W.-H. Li, C. Moroney, D. J. Diner, J. V. Martonchik, and E. Fishbein (2007a). Aerosol source plume physical characteristics from space-based multiangle imaging J. Geophys. Res., 112, D11205, doi:10.1029/2006JD007647.

Kalashnikova, O.V., R. Kahn, I.N. Sokolik, and W-H. Li, 2005, Ability of multi-angle remote sensing observations to identify and distinguish mineral dust types: Part 1. Optical models and retrievals of optically thick plumes, J. Geophys. Res., doi:10.1029/2004JD004550.

Kalashnikova O. V., and R. Kahn (2006), Ability of multi-angle remote sensing observations to identify and distinguish mineral dust types: Part 2. Sensitivity data analysis, J. Geophys. Res.,111, D11207, doi:10.1029/2005JD006756.

Kinne, S., 2009. Remote Sensing Data Combinations: Superior Maps for Aerosol Optical Depth. In: Kokhanovsky, A.A. and G. de Leeuw, ed., Satellite Aerosol Remote Sensing Over Land. Springer, Berlin, pp.361-381.

Liu, Y., P. Koutrakis, and R. Kahn, 2007. Estimating PM2.5 component concentrations and size distributions using satellite-retrieved fractional aerosol optical depth: Part 1 - Development of Methods, J. Air & Waste Management Assoc. 57, 1351-1359.

Liu, Y.J.A. Sarnat, B.A. Coull, P. Koutrakis, and D.J. Jacob, 2004, Validation of MISR aerosol optical thickness measurements using Aerosol Robotic Network (AERONET) observations over the continuous United States, J. Geophys. Res., 109, doi:10.1029/2003JD003981.

Martonchik, J.V., R.A. Kahn, and D.J. Diner, 2009. Retrieval of Aerosol Properties over Land Using MISR Observations. In: Kokhanovsky, A.A. and G. de Leeuw, ed., Satellite Aerosol Remote Sensing Over Land. Springer, Berlin, pp.267-293.

Martonchik, J.V., D.J. Diner, R.A. Kahn, B.J. Gaitley, and B.N. Holben, 2004, Comparison of MISR and AERONET aerosol optical depths over desert sites, Geophys. Res. Let.,31, doi:10.1029/2004GL019807.

Martonchik, J.V., D.J. Diner, K. Crean, and M. Bull, Regional aerosol retrieval results from MISR, IEEE Trans. Geosci. Remt. Sensing 40, 1520-1531, 2002.

Martonchik, J.V., D.J. Diner, R. Kahn, M.M. Verstraete, B. Pinty, H.R. Gordon, and T.P. Ackerman, 1998. Techniques for the Retrieval of aerosol properties over land ocean using multiangle data, IEEE Trans. Geosci. Remt. Sensing 36, 1212-1227.

Moroney, C., Davies, R. and J.-P. Muller. (2002) Operational Retrieval of Cloud-top Heights Using MISR Data. IEEE Trans. Geosci. Remote Sens. 40:1532-1540.

Redemann, J., B. Schmid, J.A. Eilers, R. Kahn, R.C. Levy, P.B. Russell, J.M. Livingston, P.V. Hobbs, W.L. Smith, Jr., and B.N. Holben, 2005, Suborbital measurements of spectral aerosol optical depth and its variability at sub-satellite-grid scales in support of CLAMS, 2001, J. Atmosph. Sci., 62(4):993-1007, doi: 10.1175/JAS3387.1.

Reidmiller, D.R., P.V. Hobbs, and R. Kahn, 2006, Aerosol optical properties and particle size distributions on the east coast of the United States, derived from airborne in situ and remote sensing measurements, J. Atmosph., Sci. 63, 785-814.

Remer, L., C. Brogniez, B. Cairns, N.C. Hsu, R. Kahn, P. Stamnes, D. Tanré, and O. Torres, 2013. Ch. 8: Recent instruments and algorithms for passive shortwave remote sensing. In: J. Lenoble, L. Remer, and D. Tanré, Eds., Aerosol Remote Sensing, Springer-Praxis Publishing, pp. 390.

Russell, P.B., J.M. Livingston, J. Redemann, B. Schmid, S. Ramirez, J. Eilers, R. Kahn, A. Chu, P.K. Quinn, M.J. Rood, and W. Wang. Multi-grid-cell validation of satellite aerosol property retrievals in INTEX.ITCT.ICARTT 2004. (2007). J. Geophys. Res. 112, D12S09, doi:10.1029/2006JD007606.

Schmid B., J. Redemann, P. B. Russell, P. V. Hobbs, D. L. Hlavka, M. J. McGill, B. N. Holben, E. J. Welton, J. R. Campbell, O. Torres, R. A. Kahn, D. J. Diner, M. C. Helmlinger, D. A. Chu, C. Robles Gonzalez, and G. de Leeuw, 2003. Coordinated airborne, spaceborne, and ground-based measurements of massive, thick aerosol layers during the dry season in southern Africa, J. Geophys. Res,108(D13), 8496, doi:10.1029/2002JD002297.

Yang, Y., L. Di Girolamo, and D. Mazzoni, 2007: Selection of the automated thresholding algorithm for the Multi-angle Imaging SpectroRadiometer Camera-by-camera Cloud Mask over land, Remote Sens. Environ., 107, 159-171.

Zhao, G. and Di Girolamo, L. (2004). A Cloud Fraction versus View Angle Technique for Automatic In-Scene Evaluation of the MISR Cloud Mask. Journal of Applied Meteorology, 43, No. 6, pp. 860 869.

Zhao, G., and L. Di Girolamo, 2006: Cloud fraction errors for trade wind cumuli from EOS-Terra instruments, Geophys. Res. Lett., 33, L20802, doi:10.1029/2006GL027088.

## 8. Useful Links

- MISR web site: http://misr.jpl.nasa.gov/
- MISR Project Guide: http://eosweb.larc.nasa.gov/GUIDE/campaign_documents/misr_ov.html
- MISR Experiment Overview: http://eospso.gsfc.nasa.gov/eos_homepage/for_scientists/atbd/viewInstrument.php?instrument=19

- MISR publications page: http://misr.jpl.nasa.gov/publications/peerReviewed/
- MISR Data: Atmospheric Sciences Data Center at LARC: http://l0dup05.larc.nasa.gov/MISR/cgi-bin/MISR/main.cgi
- MISR Data Quality Statement: https://eosweb.larc.nasa.gov/sites/default/files/project/misr/quality_summaries/L2TC_Cloud_Product.pdf

## 9. Revision History

Rev 0 – 4/18/2013 – Initial release.